Doxorubicin Loading and *In Vitro* Release from Poly(alkylcyanoacrylate) Nanoparticles Produced by Redox Radical Emulsion Polymerization

Khairallah Alhareth,[1,2] Christine Vauthier,[2] Claire Gueutin,[1,2] Gilles Ponchel,[1,2] Fathi Moussa[3]

[1]*Univ Paris-Sud, Physico-chimie, Pharmacotechnie, Biopharmacie, UMR 8612, Chatenay-Malabry, F-92296*
[2]*CNRS, Chatenay-Malabry, F-92296*
[3]*Université Paris Sud, LETIAM, IUT d'Orsay, plateau de Moulon, Bâtiment 602, 91400 Orsay, France*

Received 3 March 2010; accepted 9 May 2010
DOI 10.1002/app.32789
Published online 27 July 2010 in Wiley Online Library (wileyonlinelibrary.com).

ABSTRACT: The aim of this work was to explore the capacity to load an anticancer agent Doxorubicin (Dox) on new poly(alkylcyanoacrylate) (PACA) nanoparticles prepared by redox radical emulsion polymerization (RREP). These nanoparticles present several advantages compared with the previously described PACA nanoparticles obtained by anionic emulsion polymerization (AEP). Their cytotoxicity was lower and because they do not activate the complement system, they are believed to behave like stealth nanoparticles after intravenous administration. Dox was incorporated during the preparation of the nanoparticles. However, the drug molecules were degraded by cerium IV, which is a strong oxidant agent. To avoid drug degradation, Dox must be loaded by adsorption on preformed nanoparticles. Optimal loading capacity was deduced from a Scatchard's analysis of the Dox adsorption pattern. The loading performance [Loading efficiency (LE) 74%, Loading content (LC) 3.7%], the Dox release and the amount of Dox retained by the new nanoparticles 75% were similar to those of the already well described PACA nanoparticles obtained by AEP (LE 79% and LC 4.2%, drug retention capacity 75%). It can be concluded that the loading and releasing properties make the new nanoparticles an interesting carrier candidate for the *in vivo* delivery of Dox. © 2010 Wiley Periodicals, Inc. J Appl Polym Sci 119: 816–822, 2011

Key words: nanoparticles; poly(alkylcyanoacrylate); doxorubicin; drug delivery system; redox radical; emulsion polymerization

INTRODUCTION

Many types of nanoparticles have been designed as drug carriers with the objective of optimizing the delivery of active molecules *in vivo*, hence improving the therapeutic index of the drug. Poly(alkylcyanoacrylate) (PACA) nanoparticles are considered as the most promising biodegradable polymeric drug carriers for drug targeting.[1–4] The first PACA nanoparticles were prepared by anionic emulsion polymerization of alkylcyanoacrylate in the presence of dextran (AEP-PACA).[5] They were reported to accumulate massively in the liver and the spleen a few minutes after intravenous administration.[6–8] As nanoparticle interactions with circulating proteins and nanoparticle biodistribution depend on their surface properties,[9–12] a new method of synthesis of PACA nanoparticles by redox radical emulsion polymerization (RREP) was developed in our laboratory.[13,14] The surface of RREP-PACA nanoparticles can be modulated by the nature, and the molecular weight of the polysaccharide used as stabilizer of the polymer colloids. More interestingly, the polysaccharide chain conformation stranded at the nanoparticle surface was modified with the new method of polymerization.[15] This discrete modification of the structure of the nanoparticle polysaccharide coating induced a dramatic change of the nanoparticle properties when they are brought in contact with biological systems. For instance, the cytotoxicity of the new nanoparticles was reduced by a factor of 20 compared with that of the AEP-PACA nanoparticles.[16] The capacity of the new nanoparticles to activate the complement system was low and opposite to that shown by AEP-PACA nanoparticles.[17] With such a low capacity of complement activation, it is believed that the new nanoparticles are a good candidate to be stealth after intravenous administration, whereas the AEP nanoparticles are massively taken up by the macrophages of the reticulo-endothelial system.[18] Another advantage is found in the method of preparation, which provides with a nanoparticle suspension 10 times more concentrated than a suspension obtained by the AEP method. Thus, it will not be necessary to concentrate the nanoparticle suspension prior to *in vivo* administration, as it is often the case

Correspondence to: C. Vauthier (christine.vauthier@u-psud.fr) or F. Moussa (fathi.maussa@u-psud.fr).

considering the AEP-PACA nanoparticles. Although, a lot of work has been devoted to the physical and chemical characterization of RREP-PACA nanoparticles,[13–17] none of them have considered yet the loading and releasing capacity of these nanoparticles with an anticancer agent.

The aim of this study was to investigate the loading capacity of RREP-PACA nanoparticles with an anti cancer drug and to evaluate their releasing properties. The drug chosen for this study was Doxorubicin (Dox). This drug is among the first line anticancer agent used in clinics. As pointed out by many authors, Dox-related acute cardiotoxicity and multidrug resistance developed by cancer cells limit its use and make it an ideal candidate to be delivered by nanoparticle drug carriers.[19–21]

In this study, Dox loading capacity of the RREP-PACA nanoparticles was investigated by incorporation in the preparation medium and by adsorption on preformed nanoparticles. The releasing properties were evaluated by incubation of the Dox-loaded nanoparticles in Phosphate Buffer Saline Solutions (PBS). All results were compared with those obtained in the same conditions with Dox-loaded nanoparticles prepared according to the AEP method described in previous works.[22–25]

EXPERIMENTAL

Materials

Dextran (MW 70,000) was provided by Sigma (Saint Quentin Fallavier, France). Isobutylcyanoacrylate (IBCA) used as the monomer in the preparation of nanoparticles was a gift from Henkel Biomedical (Dublin, Ireland). Cerium IV from cerium ammonium nitrate was purchased from Fluka (Saint Quentin Fallavier, France). Doxorubicin hydrochloride was provided by Chemos GmbH (Regenstauf, Germany). Dialysis membranes (Spectra Por® cellulose ester membrane MWCO 100,000) were obtained from Carl Roth (Lauterbourg, France). All preparations were made with Milli Q® water (Waters, Saint Quentin en Yvelines, France).

MATERIALS

Redox radical emulsion polymerization

RREP was achieved as described previously.[13,14] Briefly, 0.5 mL of IBCA was added under strong magnetic stirring to 10 mL of 0.2 mol/L nitric acid containing 0.1365 g dextran (MW 70,000) and 16 mmol/L cerium IV. The nitric acid solution was purged with nitrogen for 10 min prior to the addition of the monomer and maintained at 40°C. After 1 h of polymerization, the nanoparticle suspension was rapidly cooled down in an ice bath. The nanoparticles were loaded with Dox either during preparation of the nanoparticles or by adsorption on the purified nanoparticles. In the first case, 10 mg Dox was added in the polymerization medium 1 min after the addition of the monomer, the polymerization was performed in the dark. In the latter case, the nanoparticles were prepared as described above; the suspension was purified 3 times by dialysis against Milli Q® water. The concentration of NPs was evaluated by gravimetric determination: 1 mL of the purified NPs suspensions was freeze-dried and the dry residue of the NPs was weighted. A solution of Dox in Milli Q® water (0.5 mL) at defined concentrations 0.2, 0.6, 1, 2, and 4 mg/mL was added to 0.4 mL of suspension of purified RREP-nanoparticles (10, 15, and 20 mg of nanoparticles /mL), the mixture was maintained under gentle agitation in the dark for 1 h, then the pH was adjusted to 7.4 by adding 0.1 mL of 1.0 mol/L PBS.

Anionic emulsion polymerization

The anionic emulsion polymerization was preformed as described previously.[5,22] Typically, 66.5 mg of IBCA were dropped under magnetic stirring into 6.5 mL of medium containing 5 mg of Dox, 1% dextran 70, and 0.5% citric acid. The agitation was maintained for 3 h. The polymerization occurred at room temperature. The suspension of nanoparticles was dispensed into 1.3 mL parts for lyophilization and then stored at 4°C. Resuspension of solid nanoparticles was performed by adding 1 mL of 0.1 mol/L PBS to each vial containing 13.3 mg of polymer and 1 mg of Dox.

Kinetic of cerium IV consumption

In the redox radical polymerization method, cerium IV ions are consumed during an initial reaction with dextran to produce the radicals responsible for the polymerization initiation. As the monomer is not directly involved in the chemical reaction with cerium IV, the experiment was performed in the same experimental conditions as those described for the RREP except that the monomer was not added to keep the system transparent for absorbance measurements. About 200 μL were sampled from the reaction medium at various times from 0 to 40 min. The absorbance of each sample was measured at 330 nm using a UV-spectrophotometer (UV-160A, Shimadzu). The linearity of the calibration curves was validated with aqueous solutions of cerium IV in the appropriate concentration range (0.1–1 mmol/L, $r^2 = 1$, $y = 1.4\,x - 0.05$).

Particle size and zeta potential of the nanoparticles

The mean diameter of the nanoparticles was estimated at 25°C by quasi-elastic light scattering using a Nanosizer N4 (Beckman-Coulter) operating at the

angle of 90°C. The samples were diluted in Milli Q® water by 1/400 (v/v). The results were expressed as the average of the mean hydrodynamic diameter of the dispersed particles obtained from three determinations. The standard deviation of the size distribution and the polydispersity index were also given.

The electrostatic surface charge of the polymer particles was deduced from the electrophoretic mobility using a Malvern Zetasizer nano ZS (Malvern Instruments, Uk). Dilution of the suspensions [1/200 (v/v)] was preformed in 1 mmol/L NaCl.

HPLC determination of Dox

The amount of Dox was measured by HPLC by using a Waters LC Module 1 HPLC system connected to a C_{18} column (Uptisphere C_{18}, 3 μm, 4 mm × 150 mm, Interchim), operating at 30°C, coupled with a Waters 470 Scanning Fluorescence Detector. The mobile phase consisted in a mixture of pH 2.5, 0.05*M* trichloro-acetic acid (TCA) and acetonitrile (63/37, v/v), used at a flow rate of 0.8 mL/min. Analysis were carried out at an excitation wavelength of 480 nm and an emission wavelength of 558 nm. The HPLC system was calibrated with fresh solutions of Dox. The linearity was validated with solutions of doxorubicin hydrochloride in the appropriate concentration range (0.1 to 20.0 μg/mL; $r^2 = 0.99$, $y = 673\ x + 4$).

Evaluation of Dox loading

The amount of Dox associated with the nanoparticles was determined by HPLC. The total amount of Dox (Dox_{Tot}) in nanoparticle suspension was evaluated after dissolution of the nanoparticles in DMSO (1/40, v/v). The amount of drug nonassociated with the nanoparticles (Dox_{Free}) was determined from the supernatant after removing the nanoparticles from the sample by ultracentrifugation at 61,500 *g* for 30 min.

The amount of drug associated (Dox_{Ass}) with the nanoparticles was calculated as follows:

$$Dox_{Ass} = Dox_{Tot} - Dox_{Free} \tag{1}$$

The drug loading content LC% and loading efficiency LE% were obtained by eqs. (2) and (3), respectively. (Where W_{Np} represents the weight of the nanoparticles)

$$LC\% = \left(\frac{Dox_{Ass}}{W_{Np}}\right) \times 100 \tag{2}$$

$$LE\% = \left(\frac{Dox_{Ass}}{Dox_{Tot}}\right) \times 100 \tag{3}$$

Evaluation of drug-release

In vitro release of Dox from the nanoparticles was evaluated under sink conditions: Dox concentration in the releasing medium was kept 10 times lower than the saturation solubility of Dox in PBS. A 20 μL of suspension of Dox-loaded nanoparticles was dispersed into 2.0 mL of PBS. Assuming that the total amount of Dox associated with the nanoparticles will be released, it can be calculated that the concentration of Dox expected in the total volume of the releasing medium will be 30 times less than the solubility's limit of Dox in this medium. A vial was prepared for each time point, protected from light and kept under gently stirring and controlled temperature 25°C. At predetermined time intervals, the entire release medium was ultracentrifuged at 61,500 *g* for 30 min at 25°C, and the released Dox was evaluated in the supernatant using the above described HPLC method.

Statistics and scatchard analysis

The statistical tests and the Scatchard analysis were applied using a computer software (GraphPad PRISM version 5.0). The Mann-Whitney test was applied to compare the potential Zeta of unloaded and Dox-loaded nanoparticles. The ANOVA test was used to compare their release profiles. The theoretical adsorption curve was calculated according to eq. (4), the theoretical values of number of sites (maximum mole number of Dox adsorbed on a nanoparticle) (B_{max}) and the equilibrium constant of dissociation (Kd) were estimated from the Scatchard analysis.

$$Dox_{Ass} = \frac{Dox_{Tot} \times B_{max}}{Dox_{Tot} + Kd} \tag{4}$$

The equilibrium constant of Dox adsorption K_{ads} was calculated from eq. (5).

$$K_{ads} = \frac{1}{Kd} \tag{5}$$

RESULTS AND DISCUSSION

Encapsulation of Dox by incorporation during the polymerization of the nanoparticles

At first, we attempted to encapsulate Dox in the RREP-PACA nanoparticles by adding the drug during the polymerization step. Dox was added 1 min after the beginning of the polymerization to avoid possible initiation of the polymerization on the nucleophilic groups of Dox. The total amount of drug found at the end of the polymerization step was only 10–13% of the weight of the feed, indicating that most of the drug was lost during the polymerization. This lost can be explained by the

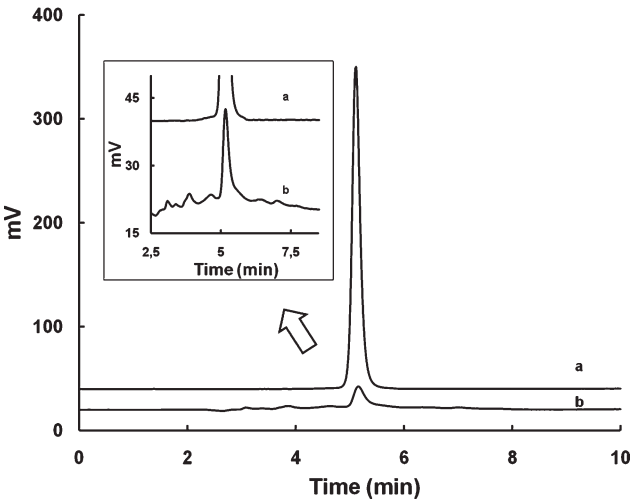

Figure 1 Chromatographic profile of Dox in the medium of polymerization at 1mg/mL: (a) before and (b) after 60 min of adding cerium IV.

degradation of Dox in the polymerization medium, because of the presence of cerium IV, which is a strong oxidant agent. This hypothesis was confirmed by the appearance in the chromatogram of additional peaks attributable to Dox degradation products[26] concomitantly with the decrease of the area of the peak attributed to Dox (Fig. 1). The cerium IV ions are part of the redox system involved in the initiation of the polymerization reaction. They react with dextran to produce radicals, which in turn initiate the polymerization of the IBCA monomer.[14] To determine whether Dox may be preserved from degradation by adding the active molecule a few minutes later after the start of the polymerization, we have studied the kinetics of cerium IV consumption during the reaction with dextran (Fig. 2). The experiments were performed in the same conditions than those used to produce the nanoparticles except that the monomer was not added to the polymerization medium because (i) the monomer was not directly involved in the reaction leading to cerium IV consumption and (ii) to reduce the complexity of cerium IV analysis. Figure 2 shows that the concentration of cerium IV decreased exponentially to reach a plateau of very low concentration (0.3 mmol/L) after 30 min. To avoid Dox oxidation, this result suggests that Dox must be added at least 30 min after the start of the polymerization process, which is useless, because at this time the nanoparticles were already formed according to a previous work.[14]

These results show that oxidizable drug molecules can be degraded by cerium IV during polymerization compromising their incorporation in PACA nanoparticles prepared by RREP. Consequently, the loading of these nanoparticles can only be achieved on preformed nanoparticles.

Association of Dox with preformed RREP-PACA

The association of Dox with RREP-PACA nanoparticles was investigated by adsorption on the preformed nanoparticles. Several concentrations of Dox were added to suspensions of nanoparticles at fixed concentrations. The limit of solubility of Dox in PBS under the same conditions than those used for the adsorption study was determined. Under our conditions, the solubility limit of Dox in PBS at pH = 7.4 was found to be 0.32 mg/mL in agreement with values found in the literature.[27] Figure 3(a) shows the concentration of Dox found in supernatants collected after ultracentrifugation of the nanoparticle suspensions incubated with various concentrations of Dox. All curves reached a plateau corresponding to the limit of solubility of Dox in the medium (0.32 mg/mL). Figure 3(b) shows that the amount of Dox in the pellet increases slowly to reach a plateau followed by a rapid increase corresponding to the precipitation of the drug in the medium. To define the formulations in which there is no precipitation, the data were analyzed according to Scatchard's formalism as previously described.[28] The Scatchard data analysis shows that the most interesting correlation was obtained from preparations of nanoparticles ranging in the zone delimited by the rectangle drawn on Figures 3(a–c). Table I summarizes the equilibrium constant dissociation and the parameters of Scatchard analysis for this group of formulations. The equilibrium constant of Dox adsorption (K_{ads}) was $0.76\times 10^{+6}$ $mol^{-1.}$ This value shows that RREP-PACA nanoparticles have important capacity of Dox adsorption.

Considered together these results allow defining the formulations in which there is no precipitation of Dox. From data of this group of formulations, the

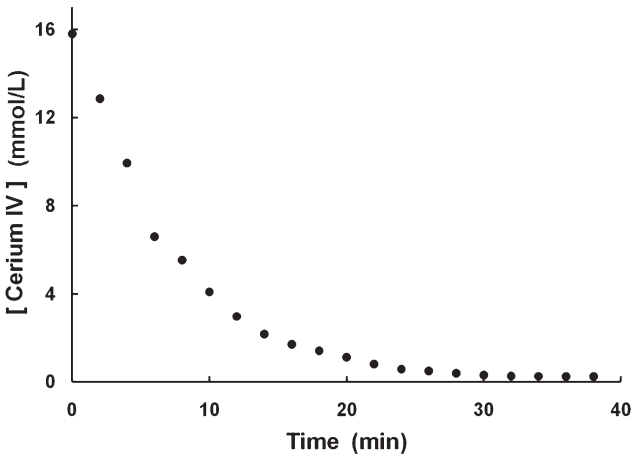

Figure 2 Kinetics of cerium IV consumption during the polymerization step.

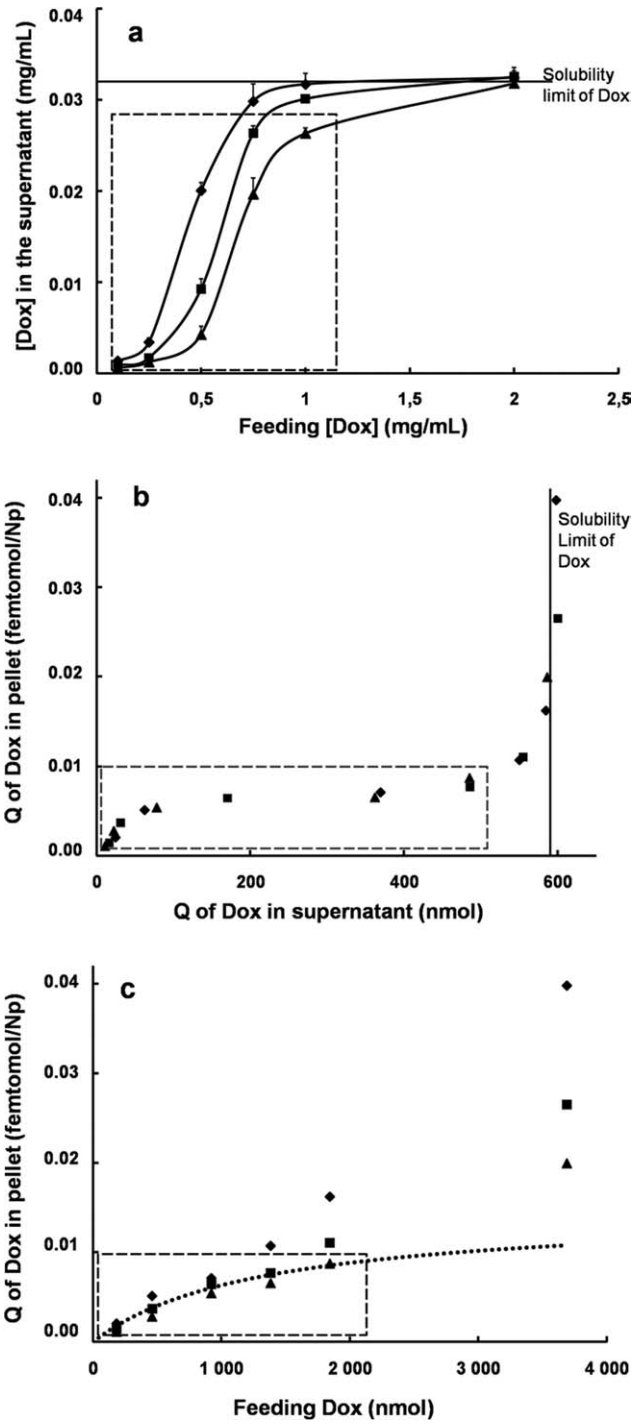

Figure 3 (a) Concentration plots of Dox in the supernatant as a function of the feeding concentration. The amount of Dox in the pellet (b) as a function of the amount of Dox in the supernatant, and (c) as a function of the amount of feeding Dox, the doted line is the calculated adsorption curve estimated from the Scatchard analysis. (◆) RREP-NPs 10 mg/mL, (■) RREP-NPs 15 mg/mL, (▲) RREP-NPs 20 mg/mL. The frame in each figure indicated the conditions under which there is no precipitation of Dox.

drug loading content (LC%) and loading efficiency (LE%) were calculated and summarized in Table II. These data clearly indicated that the optimal formulation corresponded to a concentration of nanoparticles of 20 mg/mL and an initial concentration of Dox of 1 mg/mL. This formulation showed a LC of 3.7% and a LE of 74%. For comparison, LC and LE were also determined for a preparation of PACA nanoparticles obtained by anionic emulsion polymerization in which the Dox was added during the polymerization step as previously described.[22] For such a nanoparticle suspension, the LC was found to be 4.2% and the LE was determined as 79%. The results obtained in this study were similar to those reported for AEP-PACA nanoparticles by other authors.[23] The slight difference in loading between the two types of nanoparticles can be attributed to the type of interactions between Dox and the nanoparticles. According to Henry-Toulmé et al.,[28] association of Dox with AEP-PACA nanoparticles can occur by both surface adsorption and entrapment in the core when Dox was added during the polymerization process. In contrast, when Dox is added to preformed nanoparticles, the drug can only load on particles by surface adsorption phenomenon. The loading method of the RREP-PACA nanoparticles consisted on the addition of Dox on the preformed nanoparticles. Thus the loading can only be achieved by a surface adsorption phenomenon. By comparing the results obtained with the AEP-PACA nanoparticles with those obtained with the RREP-PACA nanoparticles, it can be suggested that Dox interactions with the AEP-PACA nanoparticles were mostly based on a surface adsorption mechanism. It is noteworthy that, the values of LE and LC found for the Dox-loaded RREP-PACA nanoparticles were of the same level of those reported for other types of polymeric nanoparticles.[29–33]

Characterization of the Dox-loaded RREP-PACA nanoparticles

The optimized formulation of Dox-loaded RREP-PACA nanoparticles was characterized from its size and zeta potential. The mean diameters of the Dox-loaded nanoparticles did not differ from that of the unloaded-RREP-PACA nanoparticles (Table III). In contrast, the zeta potential of the RREP-PACA nanoparticles was significantly ($p = 0.008$) affected by the loading with Dox. Indeed, the unloaded nanoparticles showed a marked negative charge in agreement with previous reports.[13,14] This charge is attributed to the presence of dextran on the nanoparticle surface. After loading with Dox, the zeta potential of the nanoparticles was raised to reach a slightly positive value, which was in agreement with the fact that Dox is positively charged at a neutral pH. This result indicated that ionic interactions were involved in the mechanism of Dox adsorption on the nanoparticle surface.

TABLE I
Parameters of the Scatchard Analysis

K_{ads} (mol^{-1})	$0.79\times 10^{+6}$
Kd (nmol)	1315 ± 262
Bmax (femtomol/Np)	0.015 ± 0.002
95% Confidence Interval (Kd)	783–1847
95% Confidence Interval (Bmax)	0.011–0.018
r^2	0.92
Degrees of Freedom	34

Evaluation of drug-releasing properties

Release studies were preformed on the optimal formulation of Dox-loaded RREP-PACA nanoparticles. For comparison, the same experiments were also preformed with Dox-loaded AEP-PACA nanoparticles. The experiments were carried out *in vitro* using PBS as releasing medium and under sink conditions. Figure 4 shows the releasing curves obtained with the two types of nanoparticles. The releasing profile given by the RREP-PACA nanoparticles was superimposed with that of the AEP-PACA nanoparticles indicating that the two types of nanoparticles displayed the same releasing properties ($p = 0.61$). Although this was unexpected because the loading methods were different, this result agreed with our previous assumption that the major part of Dox was associated with both types of nanoparticles by surface adsorption. The released curves can be decomposed in 2 parts: 1- a controlled release part lasting for ~ 2 h and allowing the release of 25% of the drug payload and 2- a plateau indicating that a large part of the drug payload (75%) remained associated with the formulation after 6 h of incubation in PBS under sink conditions. As indicated in the first part of this work, the total amount of drug associated with the nanoparticles can be released intact when the nanoparticles are degraded. Therefore, it can be assumed that the part of Dox remaining associated with the nanoparticles can be released *in vivo* under the control of the degradation of the nanoparticles by the esterases.[34] It is noteworthy that, the releasing curves did not show a burst release of Dox. This result was rather unexpected because drug-nanoparticle association was based on surface adsorption phenomena, which are generally believed to lead to low association stability. It is also in contrast with what is observed with many types of nanoparticles due to the tremendous exchanged surface developed by such drug delivery devices with the surrounding medium.[30] However, this is an advantage because it indicated that the encapsulated drug is only released under controlled conditions. Although unexpected, this result agreed with previous finding by Liu et al.[35] According to these authors, Dox can be retained by the dextran corona of the nanoparticles thanks to the establishment of ionic interactions between the positive charge of the Dox and the negative charges of the nanoparticle surface attributed to the presence of dextran.

TABLE II
Loading Efficiency (LE) and Loading Content (LC) of Dox-Loaded RREP-PACA nanoparticles. The Values Were Not Determined (ND) for the Formulations in which There Was Dox Precipitation

RREP-NPs (mg/mL)	Dox (mg/mL)	LE%	LC%
10	0.1	87 ± 3	0.87 ± 0.03
	0.25	86 ± 2	2.16 ± 0.05
	0.5	60 ± 2	3.00 ± 0.09
	0.75	ND	ND
	1	ND	ND
	2	ND	ND
15	0.1	91 ± 1	0.61 ± 0.01
	0.25	93 ± 1	1.55 ± 0.01
	0.5	82 ± 2	2.72 ± 0.07
	0.75	65 ± 1	3.24 ± 0.05
	1	ND	ND
	2	ND	ND
20	0.1	94 ± 0.3	0.47
	0.25	95 ± 0.6	1.19 ± 0.01
	0.5	91 ± 2	2.29 ± 0.05
	0.75	74 ± 2	2.77 ± 0.09
	1	74 ± 0.6	3.68 ± 0.03
	2	ND	ND

TABLE III
Mean Diameter and Zeta Potential of the Unloaded and Dox-Loaded RREP-PACA Nanoparticles (Nanoparticles at 20 mg/mL and Dox at 1 mg/mL)

Nanoparticles	Mean diameter ± SD (nm)	PDI	Zeta potential ± SD (mV)
unloaded-RREP-PACA	291 ± 82	0.12	−8.25 ± 0.3
Dox-loaded-RREP-PACA	301 ± 82	0.04	1.1 ± 0.1

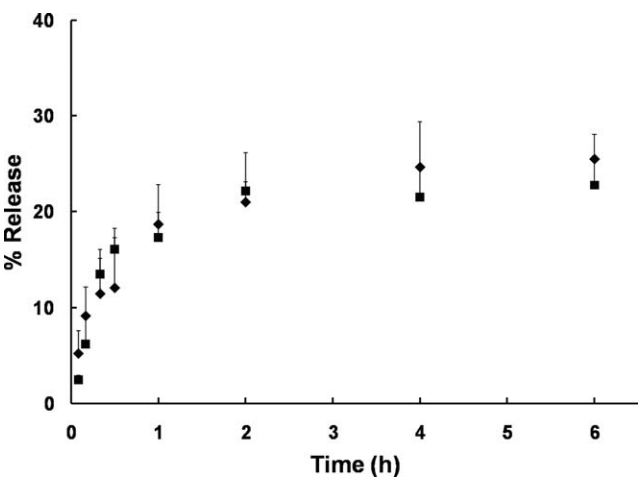

Figure 4 *In vitro* release profile of Dox in PBS (mean ± sd, n = 3) from (■) Dox-loaded RREP-PACA nanoparticles and from (◆)Dox-loaded AEP-PACA nanoparticles.

CONCLUSION

The use of a strong oxidant to initiate the redox radical polymerization compromise the loading of RREP-PACA nanoparticles with sensitive drugs like Dox by incorporation during synthesis of the drug carrier. However, this work showed that the RREP-PACA nanoparticles can be loaded with Dox by adsorption on preformed nanoparticles with the same efficacy than that previously described for the AEP-PACA nanoparticles. The releasing property of the new nanoparticles was similar to that of the AEP-PACA nanoparticles. Thanks to the stealth properties of the new RREP-PACA nanoparticles, it can be expected that the main limitation shown by the AEP-PACA nanoparticles because of their intense capture by the phagocytes of the mononuclear phagocyte system can be over passed using the new RREP-nanoparticles opening new perspectives for targeting drugs with PACA nanoparticles.

The authors thank Ministry of Health of Syria for providing Khairallah Alhareth's scholarship and Henkel Biomedical (Dublin, Ireland) for providing alkylcyanoacrylate monomer.

References

1. Vauthier, C.; Dubernet, C.; Fattal, E.; Pinto-Alphandary, H.; Couvreur, P. Adv Drug Delivery Rev 2003, 55, 519.
2. Vauthier, C.; Labarre, D.; Ponchel, G. J Drug Target 2007, 15, 641.
3. Andrieux, K.; Couvreur, P. Wiley Interdiscip Rev Nanomed Nanobiotechnol 2009, 1, 463.
4. Graf, A.; Mcdowell, A.; Rades, T. Expert Opin Drug Deliv 2009, 6, 371.
5. Couvreur, P.; Kante, B.; Roland, M.; Guiot, P.; Bauduin, P.; Speiser, P. J Pharm Pharmacol 1979, 31, 331.
6. Grislain, L.; Couvreur, P.; Lenaerts, V.; Roland, M.; Deprez-Decampeneere, D.; Speiserc, P. Int J Pharm 1983, 15, 335.
7. Lenaerts, V.; Nagelkerke, J. F.; Van Berkel, T. J.; Couvreur, P.; Grislain, L.; Roland, M.; Speiser, P. J Pharm Sci 1984, 73, 980.
8. Chiannilkulchai, N.; Ammoury, N.; Caillou, B.; Devissaguet, J. P.; Couvreur, P. Cancer Chemother Pharmacol 1990, 26, 122.
9. Lee, J.; Martic, P. A.; Tan, J. S. J Colloid Interface Sci 1989, 131, 252.
10. Stolnik, S.; Dunn, S. E.; Garnett, M. C.; Davies, M. C.; Coombes, A. G.; Taylor, D. C.; Irving, M. P.; Purkiss, S. C.; Tadros, T. F.; Davis, S. S. Pharm Res 1994, 11, 1800.
11. Sahli, H.; Tapon-Bretaudiere, J.; Fischer, A. M.; Sternberg, C.; Spenlehauer, G.; Verrecchia, T.; Labarre, D. Biomaterials 1997, 18, 281.
12. Passirani, C.; Barratt, G.; Devissaguet, J. P.; Labarre, D. Pharm Res 1998, 15, 1046.
13. Chauvierre, C.; Labarre, D.; Couvreur, P.; Vauthier, C. Pharm Res 2003, 20, 1786.
14. Bertholon-Rajota, I.; Labarre, D.; Vauthier, C. Polymer 2005, 46, 1407.
15. Bertholon, I.; Hommel, H.; Labarre, D.; Vauthier, C. Langmuir 2006, 22, 5485.
16. Chauvierre, C.; Leclerc, L.; Labarre, D.; Appel, M.; Marden, M. C.; Couvreur, P.; Vauthier, C. Int J Pharm 2007, 338, 327.
17. Bertholon, I.; Vauthier, C.; Labarre, D. Pharm Res 2006, 23, 1313.
18. Vonarbourg, A.; Passirani, C.; Saulnier, P.; Simard, P.; Leroux, J. C.; Benoit, J. P. J Biomed Mater Res A 2006, 78, 620.
19. Henderson, I. C.; Frei, E. Am Heart J 1980, 99, 671.
20. Speth, P. A.; Van Hoesel, Q. G.; Haanen, C. Clin Pharmacokinet 1988, 15, 15.
21. Reddy, L. H. J Pharm Pharmacol 2005, 57, 1231.
22. Verdun, C.; Couvreur, P.; Vranckx, H.; Lenaerts, V.; Roland, M. J Controlled Release 1986, 3, 205.
23. Soma, C. E.; Dubernet, C.; Bentolila, D.; Benita, S.; Couvreur, P. Biomaterials 2000, 21, 1.
24. Barraud, L.; Merle, P.; Soma, E.; Lefrancois, L.; Guerret, S.; Chevallier, M.; Dubernet, C.; Couvreur, P.; Trepo, C.; Vitvitski, L. J Hepatol 2005, 42, 736.
25. Pereverzeva, E.; Treschalin, I.; Bodyagin, D.; Maksimenko, O.; Langer, K.; Dreis, S.; Asmussen, B.; Kreuter, J.; Gelperina, S. Int J Pharm 2007, 337, 346.
26. Missirlis, D.; Kawamura, R.; Tirelli, N.; Hubbell, J. A. Eur J Pharm Sci 2006, 29, 120.
27. Fritze, A.; Hens, F.; Kimpfler, A.; Schubert, R.; Peschka-Suss, R. Biochim Biophys Acta 2006, 1758, 1633.
28. Henry-Toulmé, N.; Decout, A.; Lalanne, J.; Nemati, F.; Dubernet, C.; Dufourcq, J. J Colloid Interface Sci 1994, 162, 236.
29. Betancourt, T.; Brown, B.; Brannon-Peppas, L. Nanomedicine (Lond) 2007, 2, 219.
30. Park, J.; Fong, P. M.; Lu, J.; Russell, K. S.; Booth, C. J.; Saltzman, W. M.; Fahmy, T. M. Nanomedicine 2009, 5, 410.
31. Gou, M.; Zheng, X.; Men, K.; Zhang, J.; Zheng, L.; Wang, X.; Luo, F.; Zhao, Y.; Zhao, X.; Wei, Y.; Qian, Z. J Phys Chem B 2009, 113, 12928.
32. Yu, J. M.; Li, Y. J.; Qiu, L. Y.; Jin, Y. J Pharm Pharmacol 2009, 61, 713.
33. Cho, J.; Park, W.; Na, K. J Appl Polym Sci 2009, 113, 2209.
34. Muller, R. H.; Lherm, C.; Herbort, J.; Couvreur, P. Biomaterials 1990, 11, 590.
35. Liu, Z.; Cheung, R.; Wu, X. Y.; Ballinger, J. R.; Bendayan, R.; Rauth, A. M. J Controlled Release 2001, 77, 213.